

Supplementary material for

Synthesis of double core chromophore-functionalized nanothreads by compressing azobenzene in a Diamond Anvil Cell

Sebastiano Romi,^a Samuele Fanetti,^{a,b,*} Frederico Alabarse^c, Antonio M. Mio^d, Roberto Bini^{a,b,e,*}

^a*LENS, European Laboratory for Non-linear Spectroscopy, Via N. Carrara 1, I-50019 Sesto Fiorentino, Firenze, Italy*

^b*ICCOM-CNR, Istituto di Chimica dei Composti OrganoMetallici, Via Madonna del Piano 10, I-50019 Sesto Fiorentino, Firenze, Italy*

^c*ELETTRA, Elettra Sincrotrone Trieste S.C.p.A, in AREA Science Park 34149 Basovizza, Trieste, Italy*

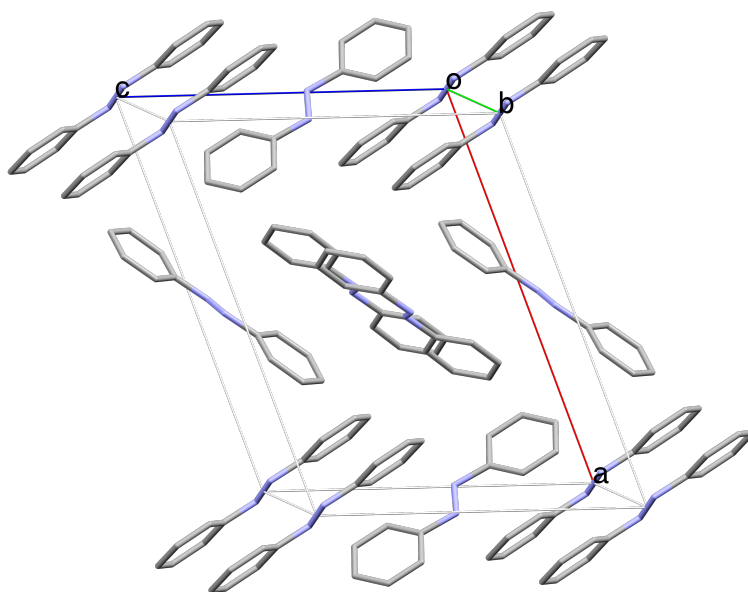
^d*IMM-CNR, Istituto per la Microelettronica e Microsistemi, VIII Strada 5 - Zona Industriale 95121 Catania, ITALY*

^e*Dipartimento di Chimica "Ugo Schiff", Università di Firenze, Via della Lastruccia 3, I-50019 Sesto Fiorentino, Italy*

^{*}*Corresponding authors: roberto.bini@unifi.it; fanetti@lens.unifi.it*

SI1: Ambient pressure crystal structure of azobenzene crystal

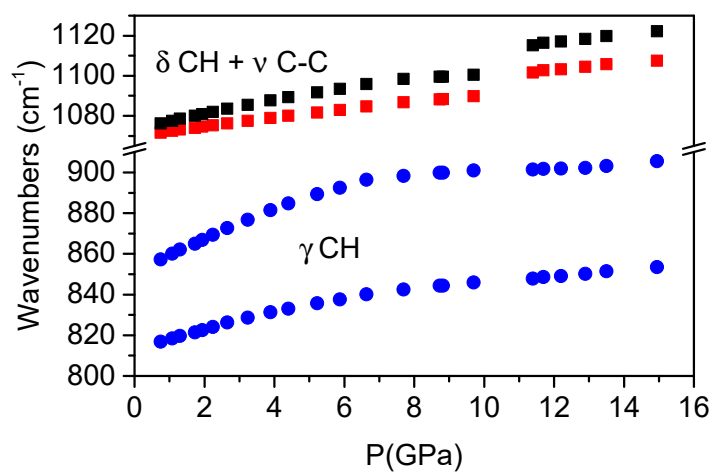
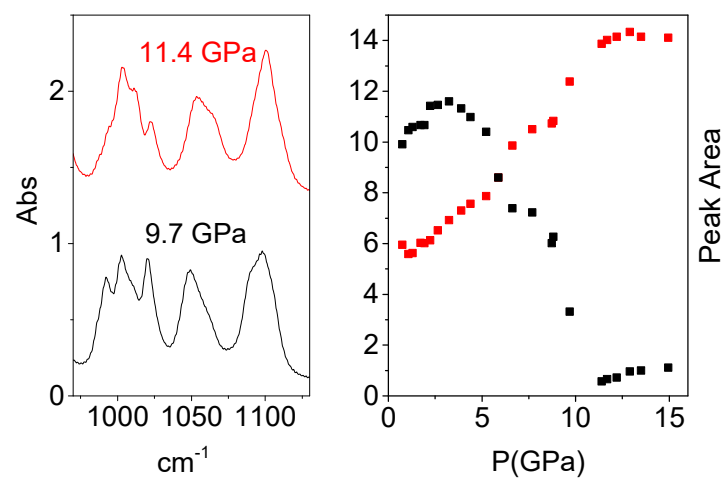
The ambient pressure crystal structure is monoclinic $P2_1/a$ containing in the asymmetric unit cell two molecules lying at inversion centers.¹ This structure is reported in the Figure below choosing a point of view which emphasizes the arrangement of equivalent molecules along the b axis. These molecules are indeed, among the equivalent ones i.e. parallel arranged, the ones showing the shortest distance between the centers of mass (5.756 Å at ambient conditions) thus representing the potential direction of the thread formation.



SI2: Spectral changes occurring in the IR spectrum before the reaction onset

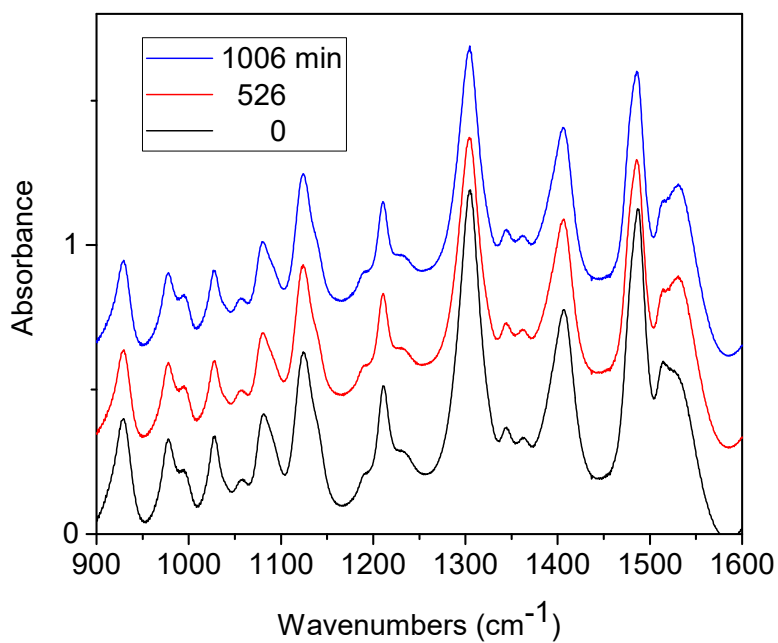
The changes observed during the compression of the azobenzene crystal in selected regions of the IR absorption spectrum are reported in the figure below. In the lower panel the pressure shift of the Davydov components of two selected vibrational modes (out of plane CH bending and mixed C-C stretching and in plane bending)² is shown. In the upper right panel we report the evolution with pressure of the mixed C-C stretching and in plane bending Davydov components absorption (same symbols as in the lower panel), whereas in the left upper panel the spectral change occurring at the frequency discontinuity around 10 GPa visible in the lower panel is shown.

The changes observed during the compression of the azobenzene crystal in selected regions of the IR absorption spectrum are reported in the figure below. In the lower panel the pressure shift of the Davydov components of two selected vibrational modes (out of plane CH bending and mixed C-C stretching and in plane bending)² is shown. In the upper right panel we report the evolution with pressure of the mixed C-C stretching and in plane bending Davydov components absorption (same symbols as in the lower panel), whereas in the left upper pane the spectral change occurring at the frequency discontinuity around 10 GPa visible in the lower panel is shown.



SI3: Kinetic analyses

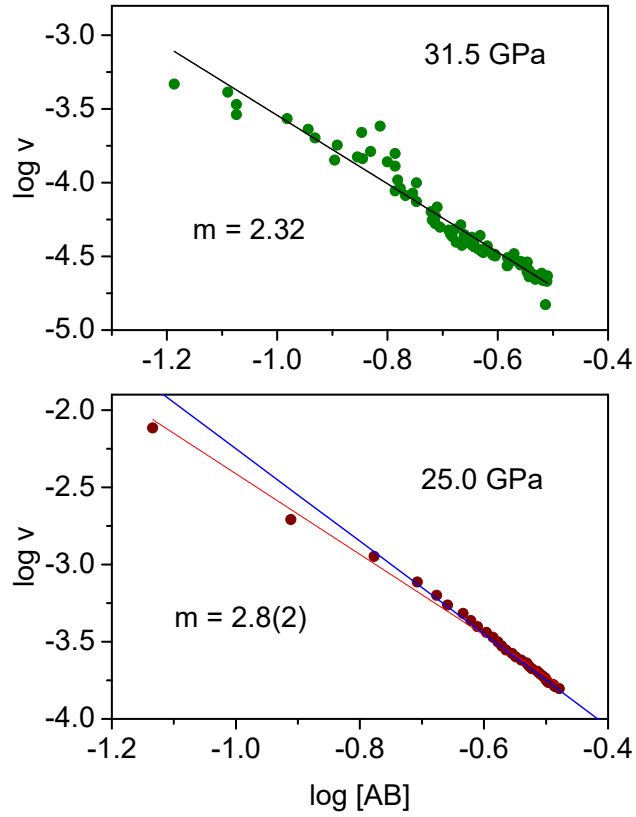
In the spectrum reported below the portion of the spectrum employed to follow the reaction kinetics is shown. The black trace is the first spectrum measured in the kinetics studied at ambient temperature and 25 GPa, the other two spectra have been measured after the time delay (minutes) reported in the legend.



SI4: Reaction Molecularity

The molecularity of the reactions has been determined using a simple kinetic relation in which the reaction rate v is assumed proportional to the azobenzene concentration $[AB]$ through the rate constant k and the process' molecularity m .³

$$v = k [AB]^m. \quad (1)$$



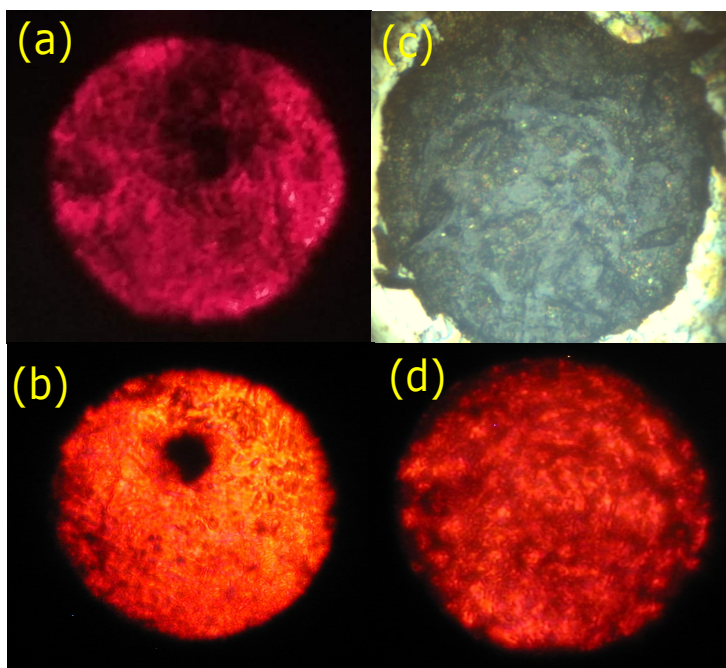
This kinetic law is generally analyzed through the following log-log relation:

$$\log(v) = m \log [AB] + \log(k). \quad (2)$$

The time evolution of the monomer concentration was reproduced by a stretched exponential in order to have an analytical function for calculating at any time the corresponding reaction rate value. In the Figure above we report the log-log plot for the two ambient temperature reaction where we performed the kinetic study. In both cases the full range of data is nicely reproduced by a single straight line whose slope indicates, according to the equation 2, a molecularity value ranging between 2.3 and 3.0 which is consistent with a rate limiting step involving two species (molecules and/or oligomers) and therefore with a linear accretion of the product. In the case of the 25.0 GPa experiment the molecularity reduces from 3.0 (blue line) to 2.6 (red line) once the first two points of the kinetics are considered, in the inset we have therefore reported the average of these limiting values.

SI5: Pictures of the recovered materials

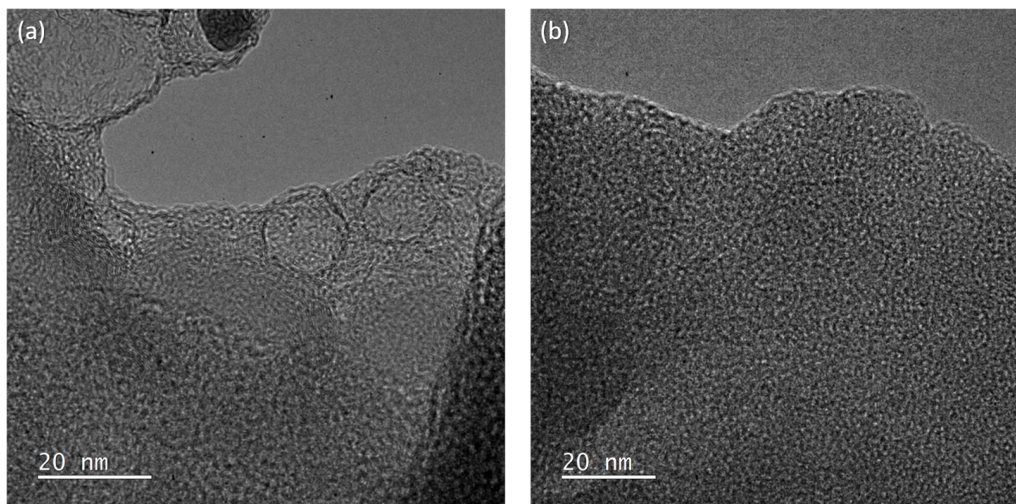
Photograph of some of the recovered materials taken after decompression. In all cases the cell was still closed therefore with a residual pressure on the sample of few GPa. The reactions were performed at the following conditions: a) 295 K and 25.0 GPa; b) 295 K and 31.5 GPa; c) 530 K and 10.0 GPa; d) 295 K and 21.7.



It is evident from the figure that all the samples produced at ambient temperature present a variable tonality of reddish coloration, on the contrary the sample produced at high temperature is completely black. It is worth remembering that this difference does not produce appreciable changes in the IR spectrum whereas, as it will be seen in the following, important modifications of the diffraction patterns are instead observed.

SI6: TEM images of amorphous sample areas

The figure reports two representative TEM images taken on different fragments showing the presence of amorphous carbon. In particular, these images have been acquired on the sample recovered from the reaction performed at ambient temperature and 25 GPa. As it can be seen, in these particular sample regions, long-range order is absent. The presence of amorphous hydrogenated carbon in the sample is expected because, as extensively discussed in the Introduction, the formation of nanothreads, eventually favoured by the anisotropic stress realized during the uniaxial compression, is never quantitative and always in competition with other reactions.

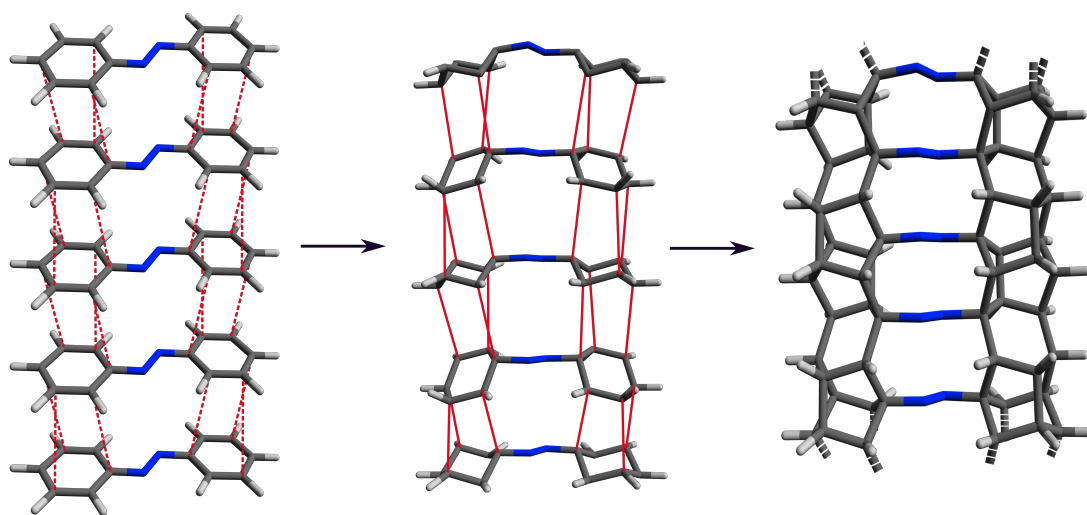


SI7: Detail of the calculation results

The DFT calculation have been performed using the RKS algorithm (Random Kitchen Sink, closed-shell Self Consistent Field calculation), the REVPBE “Revised” Perdew-Burke-Erzerhoff GGA functional, the def2-TZVPP Def2-TZVPP/C - Doubly polarized triple-zeta basis set def2 of the Karlsruhe group with “new” polarization functions with auxiliary basis set for correlation calculations. The software employed is ORCA 4.2.1, running with 4 parallel MPI-processes using open MPI 3.1.3. In the Table we report the energy data calculated for the azobenzene molecules and the two oligomers (tube(3,0) and polymer 1. All the values are in Hartree units ($1 E_h \sim 27.211$ eV).

	azobenzene	Tube (3,0)	Polymer 1
Electronic Energy (E)	-572.815292	-3443.7161194039	-3439.9867848465
Vibrational Energy	0.008460	0.0436622648	0.0429694527
Zero Point Energy	0.184274	1.3085254964	1.2199115170
Inner Energy	-572.619727	-3442.3610990999	-3438.7210713340
Enthalpy (H)	-572.618782	-3442.3601548909	-3438.7201271249
Enthropy (S)	0.049540	0.1089228031	0.1089461808
Gibbs Energy (G)	-572.668322	-3442.4690776940	-3438.8290733057
G-E	0.146970	1.24704171	1.15771154

SI8: Reaction scheme



In the figure we propose a reaction scheme leading to the polymer 1 thread structure based on the assumption of a consistent reduction of the intermolecular distance along the b axis. After para polymerization, zipping between closest rings involves adjacent not eclipsed positions (1-2', 1'-2, 5-4', 5'-4 according to the nomenclature adopted by Chen et al.⁴), these directions are indicated as dotted lines in the left picture where a stack of azobenzene molecules aligned along the b axis is considered. In the central panel the distortions caused by the new forming intermolecular bonds in the rings structure is highlighted. Finally, in the left picture we have the completion of the transformation process leading to the polymer 1 structure.

References

- [1] Brown, C. J. A Refinement of the Crystal Structure of Azobenzene. *Acta Cryst.* **1966**, *21*, 146-152.
- [2] Duarte, L.; Fausto, R.; Reva, I. Structural and spectroscopic characterization of E- and Z-isomers of azobenzene *Phys. Chem. Chem. Phys.* **2014**, *16*, 16919-16930.
- [3] Scelta, D.; Ceppatelli, M.; Bini, R. Pressure Induced Polymerization of Fluid Ethylene. *J. Chem. Phys.* **2016**, *145*, 164504.
- [4] Chen, B.; Hoffmann, R.; Ashcroft, N. W.; Badding, J.; Xu, E. S.; Crespi, V. Linearly Polymerized Benzene Arrays As Intermediates, Tracing Pathways to Carbon Nanothreads. *J. Am. Chem. Soc.* **2015**, *165*, 216-224.